

Oxygen-related defects in Si studied by variable-energy positron annihilation spectroscopy

M. Fujinami

Advanced Technology Research Laboratories, Nippon Steel Corporation, 1618 Ida, Nakahara-ku, Kawasaki 211, Japan

(Received 17 November 1995)

Variable-energy positron annihilation spectroscopy has been applied to study the behavior of oxygen-related defects in Si caused by implantation of 180-keV oxygen ions ($2 \times 10^{15}/\text{cm}^2$). In the first annealing stages of these defects ($\sim 600^\circ\text{C}$), multivacancy-oxygen complexes induced by room temperature irradiation are transformed into multivacancy-multioxygen ones in the ion-implanted region. Above 800°C , new trapping sites, where positrons are annihilated by electrons with high momentum, are created in a limited area inside the Si wafer. These defects are attributed to oxygen clusters involving several tens of oxygen atoms. The study clearly proves that positrons are a sensitive probe to detect oxygen-related defects, which are not observable by electron microscopy. [S0163-1829(96)02420-4]

An understanding of the behavior of oxygen-related defects in Si crystal is essential to the fabrication of Czochralski (CZ)-Si wafers, in which an oxygen concentration of around 10^{18} cm^{-3} is introduced from the SiO_2 crucible used in the crystal-growth process. Extensive studies on CZ-Si have been carried out, using electron-spin resonance,¹⁻³ infrared spectroscopy (IR),⁴⁻⁶ and transmission electron microscopy (TEM). Positron annihilation spectroscopy (PAS) is one of the most useful techniques to detect oxygen-related defects, as well as vacancy related defects in Si. While the interaction of positrons with both vacancies and oxygen has been studied extensively, many aspects of their behavior is not fully resolved. Dannefaer and Kerr⁷ were the first to show that interstitial oxygen clusters become active positron trapping sites. The lifetime of positrons in such sites is around 100 ps and the S parameter, characteristic of the Doppler broadening of the annihilation γ rays, is lower than that for the Si bulk. To date the defect behavior in multivacancy-multioxygen (V_xO_y) complexes in electron-irradiated⁸⁻¹⁰ and proton-irradiated¹¹ CZ-Si has been investigated using PAS and IR. It has been reported that the lifetime of the positrons trapped at V_xO_y is longer than the value of 220-ps characteristic of bulk Si, whereas the characteristic value of the characteristic S parameter for such defects strongly depends on the ratio of y to x .^{7,9,11,12} An increase in the number of oxygen coupled with these multivacancies causes the S parameter value to decrease because the fraction of the positrons annihilated by high-momentum electrons in oxygen is increased. Variable-energy positron annihilation spectroscopy (VEPAS) has been used recently as a sensitive method for depth profiling of the defect structure in Si with special application to studies of defects in the surface region.^{13,14} Coleman, Chilton, and Baker¹⁵ have investigated oxygen-related defects in p^+ -Si epilayers with various levels of oxygen incorporation using a slow positron beam. They found that when the oxygen content increases to $5 \times 10^{19}/\text{cm}^3$, the S value decreases and approaches nine tenth of the value of S for the bulk Si. The indirect recognition of oxygen-related defects in two types of ion-irradiated samples has been done by Nielsen and co-workers.^{16,17} For Si implanted with MeV Si, a low S value is observed in the damaged region after annealing above 700°C .¹⁶ The formation of a silicon-on-

insulator structure formed by high-dose ($1.7 \times 10^{18}/\text{cm}^2$) oxygen implantation to Si and subsequent annealing at high-temperature (1300°C) results in a low- S value in the top Si layer, where no oxygen precipitates are observable by TEM.¹⁷

In this work, the behavior of defects in Si induced by oxygen implantation of $2 \times 10^{15}/\text{cm}^2$ is examined by VEPAS. It is expected that excess vacancies and interstitial oxygen atoms can interact during the annealing stages, and that amorphous oxygen precipitates (SiO_x , $1.5 < x \leq 2$) and extended defects are formed ultimately. Hence, the behavior of oxygen-related defects in Si is likely to be complex and the interaction of such defects with positrons may give vital clues as to their composition.

The samples were prepared by implanting $2 \times 10^{15}\text{ O}^+$ ions/ cm^2 at 180 keV into p -type CZ-Si(100) wafers at room temperature (RT). The implantation angle was 7° from normal to the (100) face, so ion channeling is not expected to occur. Annealing of the samples from 300 – 800°C for 30 min was carried out in a nitrogen atmosphere.

The Nippon Steel Corporation slow positron beam¹⁸ was utilized to measure the Doppler broadening of the annihilation γ ray, characterized in terms of the S parameter, with respect to incident positron energy in the range 0.1–29 keV. The S parameter is defined as the ratio of the counts in a central region of the annihilation photopeak to those in the whole of the photopeak. The experimental pressure was 10^{-9} Torr and all positron measurements were taken at room temperature. The samples were subjected to an aqueous 4-vol % HF etch before measurements to remove the surface oxide and so avoid the anomalous effect of the surface silicon dioxide S parameter. Throughout this work, the S parameter is normalized to the value, S_b , for bulk silicon. The modeling and fitting program POSTRAP4 (Ref. 19) was employed for resolving the defect depth distribution from the S parameter vs incident energy (S - E) curve.

The value of the S parameter increases when the positrons are trapped at vacancy-type defects, because the overlap of the positron density with (low-momentum) valence electrons increases. When the positrons are trapped at vacancy-type defects coupled with oxygen atoms, the value of S is strongly dependent on the contribution of electrons in the oxygen

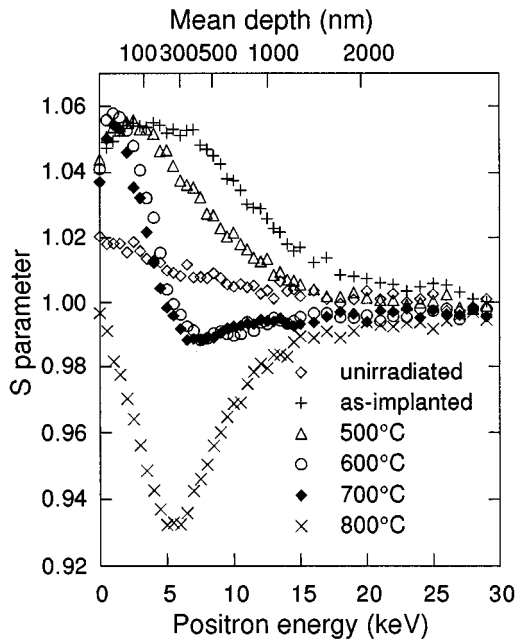


FIG. 1. S parameter vs energy (S - E) curves for the sample implanted with 2×10^{15} O ions/cm² and the samples annealed at various temperatures for 30 min in a nitrogen atmosphere.

atoms. For example, the S value of monovacancy oxygen (VO) is higher than that of the bulk Si, whereas that of VO₂ is lower.

Figure 1 shows the S - E curves of the sample implanted with 2×10^{15} O⁺ ions/cm² and the samples after annealing at various temperatures. For comparison, the S - E curve of an unirradiated Si sample, where the defect density is known to be less than the defect sensitivity limit of the positrons (5×10^{15} /cm³), is also displayed in Fig. 1. The S values for the as-implanted sample are much higher than those of the unirradiated sample, clearly indicating that vacancy-type defects are formed. In order to determine the defect profile from this S - E curve a fitting procedure, in which certain necessary parameters must be set accordingly, is necessary. These parameters are uniquely related to the type of defect that may be present in the sample and so it is important to discuss many possible defect types. Di-vacancies (V_2) are commonly known in room-temperature irradiated Si.^{20,21} It is, further, well known that oxygen is effectively bound to vacancies, forming vacancy-oxygen complexes such as VO and V₂O, which are also expected to be present in the damaged region. The characteristic values of S for all the above defects have been reported to be higher than that of bulk silicon. However, as the dominant defects produced by ion implantation is known to be V₂ based, these are the defects we initially assumed in calculating the defect profiles. Hence, for this initial analysis, a value of 3×10^{14} /s is used for the specific trapping rate (ν), and the characteristic S is held at 1.033 times that of the bulk.²² The diffusion coefficient (D_+) and the free annihilation rate (λ_b) in Si are fixed at 2.8 cm²/s and 4.5×10^9 /s, respectively. However, with these values, the fitted S - E curve could not be made to reach the peak value exhibited in the data of the experimental curve, even when the defect level in the model was set to saturation level. Higher characteristic values of S and/or spe-

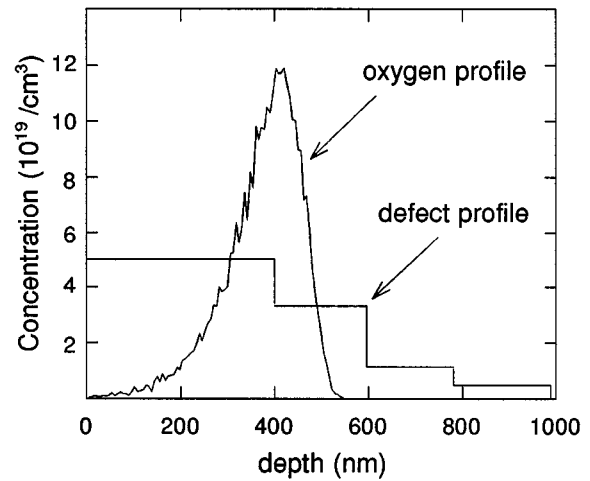


FIG. 2. The oxygen profile as calculated with TRIM and the histogram vacancy profile as derived from the S - E curve of the as-implanted samples using the POSTRAP4 program.

cific trapping rate are thus required for the fits. It has been pointed out that the relative fraction of the V_n ($n \geq 3$) defect increases with increasing damage density and that a higher S value should be used in order to fit such data.²³ Thus, the formation of V_n -based defects can be expected. For such defects, the characteristic S value may be substituted by $1.044S_b$, as was proposed by Nielsen *et al.*,¹⁶ and by using this value, the fit to the S - E curve was done well without saturation of S value. It is, hence, considered that V_n -based defects are the predominant defect induced at room temperature, and that this defect is used to fit the data, however, more detailed discussion is made later. The histogram defect profile extracted is given in Fig. 2, together with the oxygen profile derived from computer simulation using the TRIM model (transport of ions in matter).²⁴ It is found that the V_n -based defects are induced not only in the ion-projected region, but also in a deeper region up to 1 μ m. It has been reported by a number of positron-beam studies that the defect profile extends far beyond the ion-projected range, but the origin of such defects in the deeper region has yet to be clarified.²⁵⁻²⁷

No significant differences can be observed in the S - E curves upon annealing at 400 °C. However, divacancies are known to be annealed around 200 °C and transformed into multivacancies, as well as vacancy-oxygen complexes. Also, the annealing temperatures of VO and V₂O are around 350 °C and 400 °C, respectively.^{2,4,10} Therefore, if these annealing stages took place as expected, the S - E curve should change greatly in the 200–400 °C temperature range. The absence of such annealing stages suggests that the dominant defects induced at room temperature is, in fact, composed of multivacancy-oxygen complexes. As Kawasuso *et al.*¹⁰ have reported that V₃O is stable up to 500 °C, it is concluded that V_nO ($n \geq 3$) is the dominant vacancy-type defect induced by O implantation at room temperature. This result is consistent with the requirement of a high characteristic value of S for the defects as indicated by the fitting procedure explained above. Although the annealing temperature of vacancy-multioxygen defects such as VO₂ is around 500 °C,¹⁰ and so would indicate a plausible defect type, the presence of

VO_2 is discounted in the room temperature to 400 °C temperature range, because the characteristic S value for these defects is lower than that for bulk Si.

The annealing behavior of the multivacancy is now considered. According to data on electron-irradiated floating zone-Si, V_3 are found to be annealed at a temperature of less than 400 °C, giving rise to large vacancy clusters at 400 °C.²⁸ Such clusters result in the observation of a large change in S - E curves in the RT to 400 °C temperature range when multivacancies are present. Thus, the primary formation of multivacancy defects is concluded to be negligible in these samples.

After annealing at 500 °C, the first annealing stage is seen in the S - E curves beyond the ion-projected range. The value of S at high incident energy is reduced, indicating that the change in defect species is initiated from the deeper region. Annealing at 600 °C leads to an unusual S - E curve, which is unchanged upon annealing at 700 °C. A high- S value at low positron energies (<1 keV) is still observed, while the S value at energies greater than 1 keV shows a rapid decrease to a minimum value estimated to be 0.99, at 6 keV. This result strongly suggests that the annealing stage progresses from the deeper region, and that the defect species produced in the proximity of the surface are different from those in the implanted region. Above 400 °C, the multivacancy-oxygen complexes and the interstitial oxygen atoms are proposed to migrate in the implanted region and are stabilized to form more complicated multivacancy-multioxygen complexes with a lower characteristic S value than that of bulk Si. For the near surface region, it is, however, considered that the formation of large multivacancy oxygen, or vacancy clusters, is predominant. This is because the oxygen concentration is too low to produce multivacancy-multioxygen complexes.

Annealing at 800 °C results in a drastic change in the shape of the experimental S - E curve, which is then seen to be immutable upon annealing at 1000 °C: High- S values are no longer observable, indicating that vacancy-type defects disappear in the proximity of the surface, which acts as a sink. But the S - E curve does not return to that of the unirradiated Si, and a minimum value of 0.93 at positron energy 5.5 keV, where the mean implantation depth is estimated to be 260 nm, is measured. It is proposed that new trapping sites for the positrons are created in this limited area inside the Si wafer. Similar large decrease in S can be observed in the samples annealed at 800 °C after O implantations with doses of 2×10^{14} , 5×10^{14} , and $1 \times 10^{15}/\text{cm}^2$, and these S - E curves are shown in Fig. 3. It is found that each minimum value in S decreases with dose in this range. Thus, the new defects with low S are strongly related to the oxygen concentration. It is known that multivacancy-multioxygen complexes can migrate at temperatures above 800 °C,⁹ and lead to the formation of oxygen clusters and oxygen precipitates, which cause a large lowering in the S parameter. Figure 4 exhibits the cross sectional TEM micrograph of the $2 \times 10^{15}/\text{cm}^2$ implanted sample annealed at 800 °C. Oxygen precipitates and dislocations, which cannot be recognized after annealing at temperatures below 700 °C, can be observed. The oxygen precipitates are distributed from 300 to 500 nm in depth, while the dislocations are in the deeper region beyond 300 nm. It is thus considered that the positron trapping site is oxygen clusters or oxygen precipitates, al-

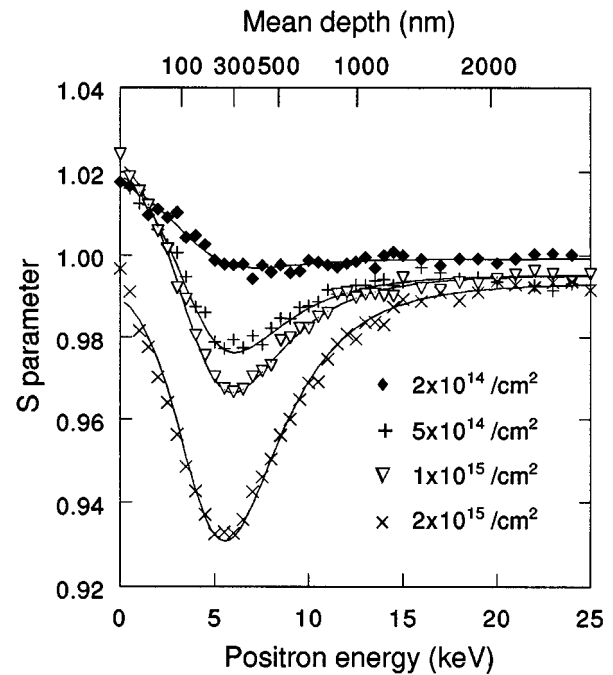


FIG. 3. S - E curves for the samples annealed at 800 °C after O implantations with 2×10^{14} , 5×10^{14} , 1×10^{15} , and 2×10^{15} O ions/ cm^2 . The solid lines are the fitted curves.

though it is very difficult between them clearly. In the four samples annealed at 800 °C, the distribution of the positron trapping sites is estimated using the transition-limited trapping model. For the fitting parameters, earlier values for λ_b , D_+ , and ν are used and the characteristic value of S for the trapping sites is taken as $0.90S_b$, as proposed by Coleman, Chilton, and Baker.¹⁵ The solid curves in Fig. 3 are the fits to the S - E curves assuming a uniform distribution of these trapping sites. The results show that they are distributed from 180 to 500 nm in depth and that no defects are

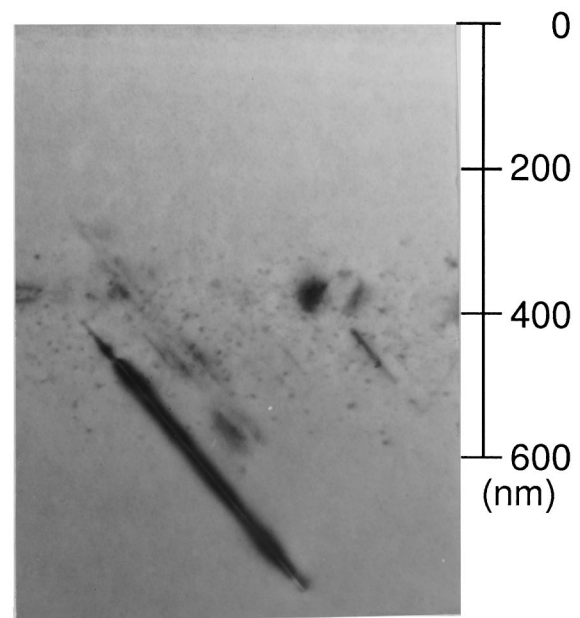


FIG. 4. Cross-sectional TEM of the 2×10^{15} O/ cm^2 implanted sample annealed at 800 °C.

present from the surface to 180-nm depth and beyond 500 nm. The distribution of oxygen precipitates observed by TEM does not correspond to that of the positron trapping sites, however. Further, although oxygen precipitates are not observable by TEM in either the 5×10^{14} sample or the 1×10^{15} cm² sample, lower S values are measured. These results indicate that oxygen precipitates cannot be the positron trapping sites. It is known that TEM observation of oxygen clusters with small size is impossible, because the minimum observable size is around 2 nm in diameter. It can be, hence, concluded that oxygen clusters with small size can be detected by positrons.

The mean number of atoms in the oxygen clusters are roughly estimated from the ratio of the density of the positron trapping sites to the atomic oxygen concentration. The former, derived from the above-mentioned fits, and the latter, calculated by TRIM in the 180–500-nm depth range, are given in Table I. The density of the oxygen clusters detected by positrons is several factors of ten lower than the average concentration of atomic oxygen. It is, therefore, speculated that several tens of oxygen atoms are involved in the oxygen clusters formed at 800 °C.

In conclusion, the author has observed the interaction of positrons with oxygen-related defects caused by implantation of 2×10^{15} O⁺/cm². The multivacancy-oxygen complexes, such as V₃O, are the primary defect found to be formed by room-temperature oxygen implantation and are stable up to 400 °C. The first annealing stage is strongly dependent on

TABLE I. The average atomic oxygen concentration from TRIM and the density of the oxygen clusters derived from the positron S - E curve at the 180–500-nm depth, for the samples implanted with different doses.

Samples (dose O/cm ²)	O (atom/cm ³)	Oxygen clusters (/cm ³)
2×10^{14}	5.9×10^{18}	1.5×10^{17}
5×10^{14}	1.4×10^{19}	7.0×10^{17}
1×10^{15}	3.0×10^{19}	1.3×10^{18}
2×10^{15}	5.9×10^{19}	3.0×10^{18}

the oxygen implantation profile and hence, the depth in the sample. In the implanted region, the formation of multivacancy-multioxygen complexes with a low characteristic S value is observed, while multivacancy-based defects are still evolved in the proximity of the surface, where the oxygen concentration is low. Upon annealing at 800 °C, the vacancy-type defects are eliminated and the multivacancy-multioxygen complexes are transformed into oxygen clusters, which have a lower S value than that of bulk Si. From the ratio of the density of oxygen clusters to the average atomic oxygen concentration, the mean number of oxygen atoms contained in the oxygen clusters is estimated to be several tens of atoms. It is clearly proven that VEPAS is very useful to detect multivacancy-multioxygen complexes and oxygen clusters, the size of which is not observable by TEM, in the surface layer.

¹G. D. Watkins and J. W. Corbett, Phys. Rev. **138**, A543 (1965).

²Y. H. Lee and J. W. Corbett, Phys. Rev. B **13**, 2653 (1976).

³K. L. Brower, Radiat. Eff. **29**, 7 (1976).

⁴B. G. Svensson and J. L. Linstrom, Phys. Rev. B **34**, 8709 (1986).

⁵H. J. Stein, Appl. Phys. Lett. **48**, 1540 (1986).

⁶D. R. Bosomworth, W. Hayes, A. R. L. Spray, and G. D. Watkins, Proc. R. Soc. London Ser. A **317**, 133 (1979).

⁷S. Dannefaer and D. Kerr, J. Appl. Phys. **60**, 1313 (1986).

⁸P. Mascher, S. Dannefaer, and D. Kerr, Phys. Rev. B **40**, 11 764 (1989).

⁹A. Ikari, H. Haga, A. Uedono, Y. Ujihira, and O. Yoda, Jpn. J. Appl. Phys. **33**, 1723 (1994).

¹⁰A. Kawasuso, M. Hasegawa, M. Suezawa, S. Yamaguchi, and K. Sumino, Appl. Surf. Sci. **85**, 280 (1995).

¹¹A. Uedono, Y. K. Cho, S. Tanigawa, and A. Ikari, Jpn. J. Appl. Phys. **33**, 1 (1994).

¹²S. Dannefaer, Phys. Status Solidi A **102**, 481 (1987).

¹³P. J. Schultz and K. G. Lynn, Rev. Mod. Phys. **60**, 701 (1988).

¹⁴P. Asoka-Kumar, K. G. Lynn, and D. O. Welch, J. Appl. Phys. **76**, 4935 (1994).

¹⁵P. G. Coleman, N. B. Chilton, and J. A. Baker, J. Phys. Condens. Matter **2**, 9355 (1990).

¹⁶B. Nielsen, O. W. Holland, T. C. Leung, and K. G. Lynn, J. Appl. Phys. **74**, 1636 (1993).

¹⁷B. Nielsen, K. G. Lynn, T. C. Leung, B. F. Cordts, and S. Seraphin, Phys. Rev. B **44**, 1812 (1991).

¹⁸M. Fujinami, Hoshasen **18**, 55 (1992).

¹⁹G. C. Aers, in *Positron Beams for Solids and Surfaces*, Proceedings of the 4th International Workshop on Slow-Positron Beam Techniques for Solids and Surfaces, edited by P. J. Schultz, G. R. Massoumi, and P. J. Simpson, AIP Conf. Proc. No. 218 (AIP, New York, 1990), p. 162.

²⁰H. J. Stein, F. L. Vook, and J. A. Borders, Appl. Phys. Lett. **14**, 328 (1969).

²¹J. W. Mayer, L. Eriksson, S. T. Picraux, and J. A. Davies, Can. J. Phys. **46**, 663 (1968).

²²R. D. Goldberg, P. J. Schultz, and P. J. Simpson, Appl. Surf. Sci. **85**, 287 (1995).

²³P. J. Simpson, M. Vos, I. V. Mitchell, C. Wu, and P. J. Schultz, Phys. Rev. B **44**, 12 180 (1991).

²⁴J. P. Biersack and L. G. Haggmark, Nucl. Instrum. Methods **174**, 257 (1980).

²⁵A. Uedono, S. Tanigawa, J. Sugiura, and M. Ogasawara, Jpn. J. Appl. Phys. **29**, 1867 (1990).

²⁶A. Uedono, L. Wei, C. Dosho, H. Kondo, S. Tanigawa, J. Sugiura, and M. Ogasawara, Jpn. J. Appl. Phys. **30**, 201 (1991).

²⁷M. Fujinami and N. B. Chilton, J. Appl. Phys. **73**, 3242 (1993).

²⁸A. Kawasuso, M. Hasegawa, M. Suezawa, S. Yamaguchi, and K. Sumino, in *Positron Annihilation*, Proceedings of the 10th International Conference on Positron Annihilation, edited by Y. J. He, B. S. Cao, and Y. C. Jean (Trans Tech, Switzerland, 1995), Vols. 175–178, p. 423.